ISSN 1063-7834, Physics of the Solid State, 2021, Vol. 63, No. 8, pp. 1159–1164. © Pleiades Publishing, Ltd., 2021.
ISSN 1063-7834, Physics of the Solid State, 2021. © Pleiades Publishing, Ltd., 2021.
Russian Text © The Author(s), 2021, published in Fizika Tverdogo Tela, 2021, Vol. 63, No. 8, pp. 1056–1061.

Synthesis, Crystal Structure, and Thermal Properties of Substituted Titanates $Bi_2Pr_2Ti_3O_{12}$ and $Bi_2Nd_2Ti_3O_{12}$

L. T. Denisova[a, *], M. S. Molokeev[a, b], N. A. Galiakhmetova[a], V. M. Denisov[a], and G. V. Vasil'ev[a]

[a] *Siberian Federal University, Krasnoyarsk, 660041 Russia*

[b] *Kirensky Institute of Physics, Krasnoyarsk Scientific Center, Siberian Branch, Russian Academy of Sciences, Krasnoyarsk, 660036 Russia*

**e-mail: ldenisova@sfu-kras.ru*

Received March 31, 2021; revised April 3, 2021; accepted April 3, 2021

Abstract—Titanates $Bi_2Pr_2Ti_3O_{12}$ and $Bi_2Nd_2Ti_3O_{12}$ have been obtained by the solid-phase synthesis using sequential annealing of the Bi_2O_3, Nd_2O_3, Pr_6O_{11}, and TiO_2 stoichiometric mixtures in air at temperatures of 1003–1323 K. Their crystal structure has been established by X-ray diffractometry and the high-temperature heat capacity has been determined by differential scanning calorimetry. Based on the experimental $C_p = f(T)$ data, the main thermodynamic functions have been calculated.

Keywords: substituted bismuth titanate, solid-state synthesis, crystal structure, high-temperature heat capacity, thermodynamic functions

DOI: 10.1134/S1063783421080084

1. INTRODUCTION

The $Bi_{4-x}R_xTi_3O_{12}$ (R is the rare-earth element, REE) solid solutions are obtained by substituting REEs for a part of bismuth in titanate $Bi_4Ti_3O_{12}$. Recently, there has been a sustainable interest in such materials. The solid solutions containing La [1–3], Ce [2], Nd [4–6], Sm [7–9], Eu [10], Er [11], Pr, Nd, Cd, and Dy [12, 13] were synthesized. The layered bismuth titanate-based solid solutions attract attention because the substitution of REEs for bismuth changes the properties (permittivity, conductivity, Curie temperature, etc.) of titanate. According to [3, 14, 15], the substitution of La for Bi reduces the fatigue and polarization of $Bi_4Ti_3O_{12}$. It is believed that such materials surpass the well-known ferroelectric lead zirconate [3] in some functional characteristics. Most studies on the substituted bismuth titanate deal with its electrical properties. This is due to the prospects of their application in acousto- and optoelectronics, piezoelectric transducers, ferroelectric memory, etc. Nevertheless, despite such attention to these materials, many of their properties have been understudied. This concern, first of all, the thermal characteristics. Some of the available data on the crystal structure of the solid solutions are contradictory. For example, it was reported in [13, 14] that the substitution of REEs for Bi preserves the orthorhombic symmetry, while in [3, 16] it was stated that it changes for tetragonal one. The phase diagrams of the $Bi_4Ti_3O_{12}$–$R_4Ti_3O_{12}$ systems have not been built. Note that, in the phase diagrams of Nd_2O_3–TiO_2 [17], Er_2O_3–TiO_2 [18], Lu_2O_3–TiO_2 [19], Bi_2O_3–TiO_2–Y_2O_3 [20], La_2O_3–TiO_2 [21], Gd_2O_3 (Dy_2O_3)–TiO_2 [22], and R_2O_3–TiO_2 (R = La, Ce, Pr, Nd, Sm, Gd, Tb, Dy, Ho, Er, Yb, Y) [23], no $R_4Ti_3O_{12}$ compounds were observed. Nevertheless, the data on their formation were reported: $Eu_4Ti_3O_{12}$ [23], $La_4Ti_3O_{12}$ [24, 25], and $Nd_4Ti_3O_{12}$ [17]. Computer modeling of these systems requires data on the thermodynamic properties of the resulting compounds. Such data are lacking in the literature, except for the simple oxides and $Bi_4Ti_3O_{12}$.

This study presents the results of the synthesis of titanates $Bi_2Pr_2Ti_3O_{12}$ and $Bi_2Nd_2Ti_3O_{12}$ and investigations of their crystal structure and thermophysical properties.

2. EXPERIMENTAL

The substituted titanates $Bi_2Pr_2Ti_3O_{12}$ and $Bi_2Nd_2Ti_3O_{12}$ were obtained by the solid-phase synthesis from the initial oxides Bi_2O_3, Nd_2O_3, and TiO_2 (of special purity grade) and Alfa Aesor Pr_6O_{11} (99.999%). To do that, the stoichiometric mixtures of the pre-calcined oxides were homogenized in a Retsch PM 100 planetary ball mill (Germany) with zirconium dioxide glasses and balls at a working vessel rotation rate of 180 rpm and a processing time of 30 min. Since the obtained powders subjected to such processing can interact with the environment [26], they were immediately placed in polyethylene containers, evacuated,

Table 1. Main experimental parameters and results of refinement for $Bi_2Pr_2Ti_3O_{12}$ and $Bi_2Nd_2Ti_3O_{12}$

Composition	$Bi_2Pr_2Ti_3O_{12}$	$Bi_2Nd_2Ti_3O_{12}$
Sp. gr.	$P4_2/nmc$	$P4_2/nmc$
a, Å	3.81590(11)	3.80943(8)
c, Å	32.7879(15)	32.7697(11)
V, Å^3	477.43(4)	475.55(3)
Z	2	2
2θ range, deg	5–120	5–120
R_{wp}, %	7.91	6.75
R_p, %	6.31	5.35
R_B, %	2.50	1.69
χ^2	1.85	1.68

a and c are the unit cell parameters; V is the cell volume; R_{wp}, R_p, and R_B are the weight profile, profile, and integral infidelity factors, respectively; and χ^2 is the fitting quality.

Table 2. Atomic coordinates and isotropic thermal parameters of the $Bi_2Pr_2Ti_3O_{12}$ and $Bi_2Nd_2Ti_3O_{12}$ solid solutions

Atom	x	y	z	B_{iso}	Occ
$Bi_2Pr_2Ti_3O_{12}$					
Bi1	0.25	0.25	0.31600(8)	0.55(11)	0.288(8)
Pr1	0.25	0.25	0.31600(8)	0.55(11)	0.712(8)
Bi2	0.25	0.25	0.46124(7)	0.30(10)	0.701(8)
Pr2	0.25	0.25	0.46124(7)	0.30(10)	0.299(8)
Ti1	0.25	0.25	0.75	0.5(3)	1
Ti2	0.25	0.25	0.6209(2)	0.50(19)	1
O1	0.75	0.75	0.2375(10)	1.1(3)	1
O2	0.75	0.75	0.4940(18)	1.1(3)	1
O3	0.25	0.25	0.6899(7)	1.1(3)	1
O4	0.25	0.25	0.5769(9)	1.1(3)	1
O5	0.75	0.75	0.3556(15)	1.1(3)	1
O6	0.75	0.75	0.1359(17)	1.1(3)	1
$Bi_2Nd_2Ti_3O_{12}$					
Bi1	0.25	0.75	0.31594(7)	0.46(11)	0.215(6)
Pr1	0.25	0.75	0.31594(7)	0.46(11)	0.785(6)
Bi2	0.25	0.75	0.46134(6)	0.30(10)	0.777(7)
Pr2	0.25	0.75	0.46234(6)	0.30(10)	0.223(7)
Ti1	0.25	0.75	0.75	0.5(3)	1
Ti2	0.25	0.75	0.6217(2)	0.50(18)	1
O1	0.75	0.75	0.2376(9)	1.3(3)	1
O2	0.75	0.75	0.4954(18)	1.3(3)	1
O3	0.25	0.75	0.6911(5)	1.3(3)	1
O4	0.25	0.75	0.5713(7)	1.3(3)	1
O5	0.75	0.75	0.3569(13)	1.3(3)	1
O6	0.75	0.75	0.1353(15)	1.3(3)	1

and sealed. After that, they were pressed using a YLJ-CIP-20B isostatic press (P = 150 MPa and τ = 5 min). The obtained samples were burnt in air for 10 h at temperatures of 1073, 1103, 1153, 1273, and 1323 K (1203 K, 20 h). After each temperature, they were ground in a planetary mill and pressed again under the same conditions. The X-ray diffraction powder patterns of the titanates $Bi_2Nd_2Ti_3O_{12}$ and $Bi_2Pr_2Ti_3O_{12}$ were recorded on a Bruker D8 ADVANCE diffractometer (CuK_α radiation) at room temperature using a VANTEC linear detector.

The heat capacity of the titanates $Bi_2Pr_2Ti_3O_{12}$ and $Bi_2Nd_2Ti_3O_{12}$ was measured by differential scanning calorimetry using a NETZSCH STA 449 C Jupiter thermal analyzer (Germany). The experimental technique was similar to that described previously in [27, 28]. The experimental error was no more than 2%.

3. EXPERIMENTAL RESULTS

All the reflections in the X-ray diffraction patterns were indexed in a $P4_2/nmc$ tetragonal cell. Therefore, this structure was taken as an initial model for the Rietveld refinement in the TOPAS 4.2 program [29]. The two Bi sites exist in the independent part of the cell and both of them were occupied with Bi/Pr and Bi/Nd ions for each phase, respectively. The occupancies of the sites were refined and, to increase the stability of the refinement, the sum of the number of Bi and Pr(Nd) ions in the cell was restricted by linear

Table 3. Main bond lengths (Å)

$Bi_2Pr_2Ti_3O_{12}$			
(Bi1/Pr1)–O1^{i}	2.59(2)	Ti1–O1^{iii}	1.952(7)
(Bi1/Pr1)–O3^{ii}	2.7051(16)	Ti1–O3	1.97(2)
(Bi1/Pr1)–O5	2.31(3)	Ti2–O3	2.26(2)
(Bi1/Pr1)–O6^{i}	2.84(4)	Ti2–O4	1.44(3)
(Bi2/Pr2)–O2	2.19(3)	Ti2–O5^{iii}	2.058(19)
(Bi2/Pr2)–O2^{iii}	2.41(4)	Ti2–O6^{iv}	1.970(14)
(Bi2/Pr2)–4O^{ii}	2.974(12)		
$Bi_2Nd_2Ti_3O_{12}$			
(Bi1/Nd1)–O1^{i}	2.589(19)	Ti1–O1^{iii}	1.948(6)
(Bi1/Nd1)–O3^{ii}	2.7036(15)	Ti1–O3	1.930(18)
(Bi1/Nd1)–O5	2.33(3)	Ti2–O3	2.274(19)
(Bi1/Nd1)–O6^{i}	2.49(3)	Ti2–O4	1.65(2)
(Bi2/Nd2)–O2	2.21(3)	Ti2–O5^{iii}	2.029(15)
(Bi2/Nd2)–O2^{iii}	2.37(4)	Ti2–O6^{iv}	1.956(11)
(Bi2/Nd2)–4O^{ii}	2.899(9)		

Symmetry elements (i) $x + 1$, $-y + 1$, $-z + 1/2$; (ii) x, $-y + 1$, $-z + 1$; (iii) $x + 1$, $-y + 1$, $-z + 1$; (iv) $x + 3/2$, $-y + 1/2$, $z + 1/2$; and (v) $x + 2$, $-y + 1$, $-z + 1/2$.

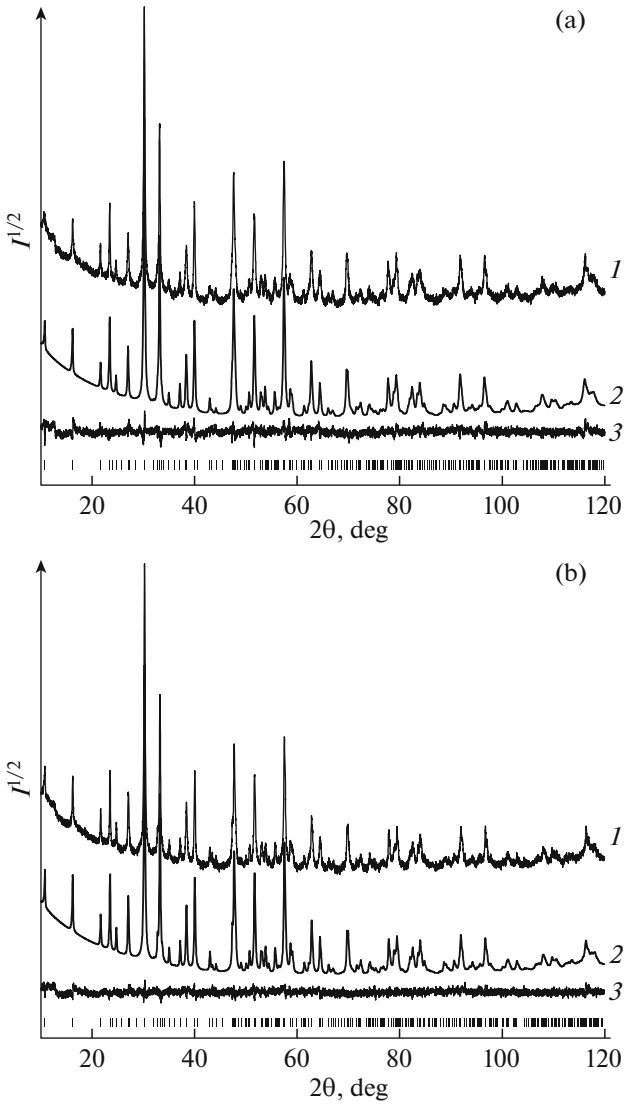

Fig. 1. (*1*) Experimental, (*2*) calculated, and (*3*) difference profiles of the X-ray diffraction patterns for (a) $Bi_2Pr_2Ti_3O_{12}$ and (b) $Bi_2Nd_2Ti_3O_{12}$ after the refinement using the derivative difference minimization method. Bars show the calculated reflection positions.

equations. As a result, the refinement of all the structures was stable and yielded low infidelity factors (Table 1). The atomic coordinates and thermal parameters are given in Table 2 and the main bond lengths, in Table 3; the difference X-ray diffraction patterns are shown in Fig. 1.

The structure of unsubstituted bismuth titanate has been studied repeatedly. The results obtained appeared contradictory. In particular, according to [11, 30], $Bi_4Ti_3O_{12}$ has a rhombic unit cell (sp. gr. *Fmmm*) at room temperature. Most authors believe that this titanate is characterized by sp. gr. *B*2*cb* [13, 14, 16] or *Aba*2 [31, 32] (obtained by the transformation from *B*2*cb* (*Aba*2 : *abc* = *B*2*cb* : *b*'*c*'*a*' [31])).

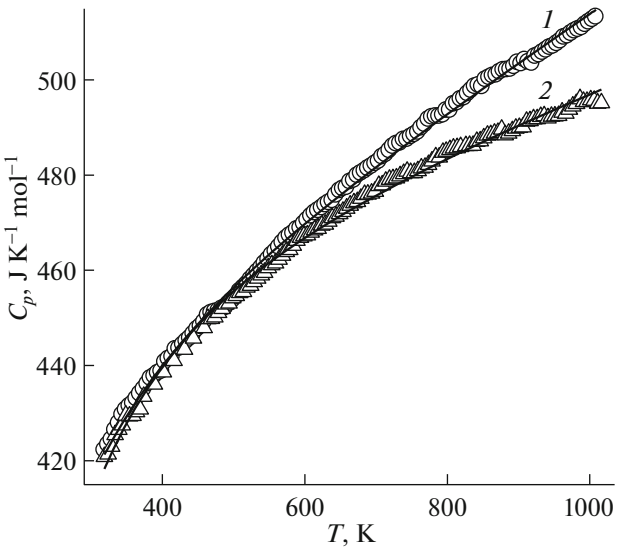

Fig. 2. Temperature dependences of the molar heat capacity for (*1*) $Bi_2Pr_2Ti_3O_{12}$ and (*2*) $Bi_2Nd_2Ti_3O_{12}$.

According to our data, $Bi_4Ti_3O_{12}$ has sp. gr. *Aba*2. These data and Table 1 show that, upon substitution of Pr or Nd for Bi, the structure changes (sp. gr. $P4_2/nmc$). According to the data from [33], the $Bi_2R_2Ti_3O_{12}$ (R = La, Pr, Nd, Sm) compounds have sp. gr. $I4/mmm$ with unit cell parameters of $a \sim 3.8$ Å and $c \sim 33$ Å. A similar situation was noted for $Bi_2Nd_2Ti_3O_{12}$ [16] and $Bi_2La_2Ti_3O_{12}$ [34]. At the same time, there are different data. According to [35], the $Bi_2La_2Ti_3O_{12}$ compound forming in the course of the reaction between $K_2La_2Ti_3O_{10}$ and BiOCl has an orthorhombic unit cell ($a = 5.441(1)$ Å, $b = 5.399(1)$ Å, and $c = 32.944(4)$ Å).

The search for a suitable phase related to the low-symmetry *Aba*2 phase by the group properties, which was carried out by us in the PSEUDO program [36], showed that the most suitable structures (the atomic displacement is smaller than 1 Å) can be two structures with sp. gr. $P4_2/nmc$ and $I4/mmm$. The test refinement for both models yielded Bragg factors *R* of 2.50% and 1.69% ($P4_2/nmc$) and 3.91% and 3.49% ($I4/mmm$) for $Bi_2Pr_2Ti_3O_{12}$ and $Bi_2Nd_2Ti_3O_{12}$, respectively. Taking into account that these values for the $P4_2/nmc$ model turned out to be noticeably smaller, as well as the fact that the numbers of the refined structural parameters for the two models are similar (8 refined coordinates for $I4/mmm$ and 9 coordinates for $P4_2/nmc$) and that the $I4/mmm$ structure had the high thermal parameters for all oxygen atoms, the $P4_2/nmc$ model was preferred.

The effect of temperature on the heat capacity of $Bi_2Pr_2Ti_3O_{12}$ and $Bi_2Nd_2Ti_3O_{12}$ is illustrated in Fig. 2. With an increase in temperature from 320 to 1000 K, the C_p values naturally increase and the dependences

Table 4. Thermodynamic properties of $Bi_2Pr_2Ti_3O_{12}$ and $Bi_2Nd_2Ti_3O_{12}$

T, K	C_p, J K^{-1} mol^{-1}	$H°(T) - H°(320\ K)$, kJ mol^{-1}	$S°(T) - S°(320\ K)$, J K^{-1} mol^{-1}	$-\Delta G/T$*, J K^{-1} mol^{-1}
$Bi_2Pr_2Ti_3O_{12}$				
320	421.7	–	–	–
350	429.4	12.87	38.14	1.65
400	440.0	34.51	96.19	9.91
450	448.7	56.74	148.5	22.45
500	456.4	79.70	196.2	37.48
550	463.3	102.4	240.0	53.93
600	469.8	125.7	280.6	71.15
650	475.8	149.3	318.5	88.73
700	481.7	173.3	354.0	106.4
750	487.3	197.5	387.4	124.1
800	492.8	222.0	419.0	141.5
850	498.2	246.8	449.1	158.7
900	503.5	271.8	477.7	175.7
950	508.7	297.1	505.0	192.3
1000	513.9	322.7	531.2	208.6
$Bi_2Nd_2Ti_3O_{12}$				
320	418.7	–	–	–
350	427.9	12.70	37.94	1.64
400	439.6	34.41	95.89	9.87
450	448.5	56.62	148.2	22.38
500	455.6	79.23	195.8	37.38
550	461.6	102.2	239.5	53.80
600	466.8	125.4	279.9	70.98
650	471.5	148.8	317.5	88.51
700	475.7	172.5	352.6	106.1
750	479.7	196.4	385.5	123.7
800	483.4	220.5	416.6	141.0
850	487.0	244.7	446.0	158.1
900	490.4	269.2	473.7	174.9
950	493.7	293.8	500.6	191.3
1000	497.0	318.5	526.0	207.4

*$\Delta G/T = [H°(T) - H°(320\ K)]/T - [S°(T) - S°(320\ K)]$.

$C_p = f(T)$ do not contain any kinds of extrema. According to the data from [37], the dependence $C_p = f(T)$ for unsubstituted bismuth titanate has an extremum in the region of the ferroelectric phase transition at 943 K, which is not observed for $Bi_2Pr_2Ti_3O_{12}$ and $Bi_2Nd_2Ti_3O_{12}$. A similar phenomenon was previously observed in studying the heat capacity of cuprates $La_{2-x}Sr_xCuO_4$ ($0 \le x \le 0.2$) [38]. As the Sr concentration increases, the extremum in the curve $C_p = f(T)$ shifts toward lower temperatures.

The experimental results on the heat capacity of $Bi_2Pr_2Ti_3O_{12}$ and $Bi_2Nd_2Ti_3O_{12}$ can be described by the Maier–Kelley equation [39]

$$C_p = a + bT - cT^{-2}, \quad (1)$$

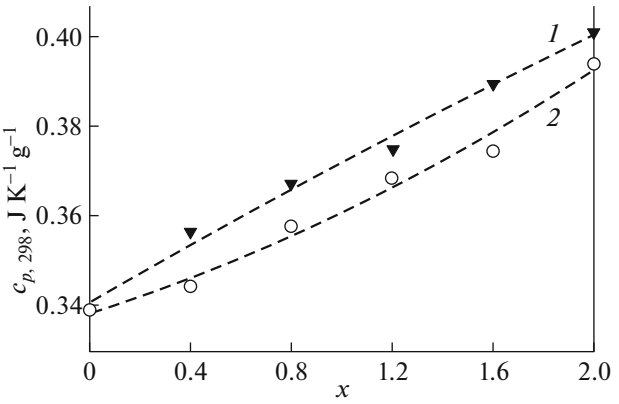

Fig. 3. Effect of the composition of the $Bi_2Pr_{2-x}Ti_3O_{12}$ (*1*) and $Bi_2Nd_{2-x}Ti_3O_{12}$ (*2*) solid solutions on their heat capacity.

which have the form

$$C_p = (419.9 \pm 1.1) + (96.90 \pm 1.2)\times 10^{-3}T - (29.99 \pm 1.05)\times 10^{5}T^{-2}, \quad (2)$$

$$C_p = (417.1 \pm 1.1) + (54.55 \pm 1.2)\times 10^{-3}T - (46.90 \pm 1.11)\times 10^{5}T^{-2} \quad (3)$$

for the investigated bismuth titanates (J K^{-1} mol^{-1}).

The correlation coefficients for Eqs. (2) and (3) are 0.9979 and 0.9982 and the maximum deviations of the experimental points from the smoothing curves are 1.17% and 1.23%, respectively.

It was impossible to compare the obtained results on the heat capacity of $Bi_2Pr_2Ti_3O_{12}$ and $Bi_2Nd_2Ti_3O_{12}$ with the data of other authors, since the latter are lacking. Therefore, we studied the effect of the composition of the solid solutions on their heat capacity (Fig. 3). To ignore the difference in molar masses, specific heats c_p are presented. It can be seen that, with an increase in the REE concentration, the c_p values at 298 K naturally increase. This is apparently indicative of the reliability of the obtained heat capacities for $Bi_2Pr_2Ti_3O_{12}$ and $Bi_2Nd_2Ti_3O_{12}$.

Using Eqs. (2) and (3), the thermodynamic functions of the substituted bismuth titanates were calculated using the available thermodynamic relations. The results are given in Table 4.

4. CONCLUSIONS

Substituted titanates $Bi_2Pr_2Ti_3O_{12}$ and $Bi_2Nd_2Ti_3O_{12}$ were obtained by the solid-phase synthesis. The crystal structure was determined and the effect of temperature (320–1000 K) on the heat capacity was investigated. The thermodynamic functions were calculated using the experimental $C_p = f(T)$ data.

ACKNOWLEDGMENTS

The authors thank the Krasnoyarsk Territorial Center for Collective Use, Krasnoyarsk Scientific Center, Siberian Branch of the Russian Academy of Sciences.

FUNDING

This study was carried out in part within the state assignment for the Siberian Federal University, project no. FSRZ-2020-0013.

CONFLICT OF INTEREST

The authors declare that they have no conflicts of interest.

REFERENCES

1. M. S. Tomar, R. E. Melgarejo, A. Hidalgo, S. B. Mazumder, and R. S. Katiyar, Appl. Phys. Lett. **33**, 341 (2003).
2. N. Pavlović, D. Kanco, K. M. Szécsénji, and V. V. Srdié, Proc. Appl. Ceram. **3**, 88 (2009).
3. A. I. Klyndyuk, A. A. Glinskaya, E. A. Chizhova, and L. A. Bashkirov, Ogneupory Tekh. Keram., Nos. 1–2, 29 (2017).
4. C. Yang, Z. Wang, D. Pan, J. Han, Q. Li, and J. Wang, Sur. Rev. Lett. **11**, 503 (2004).
5. Y.-M. Kan, G.-J. Zhang, P.-L. Wang, and Y.-B. Cheng, J. Eur. Ceram. Soc. **28**, 1641 (2008).
6. Y. Wang, N. Zhao, M. Zhang, and X. Zhao, J. Wuhan Univ. Technol.-Mater. Sci. **25**, 743 (2010).
7. M. Iwata, A. Toya, R. Aoyagi, M. Maeda, and Y. Ishibashi, Jpn. J. Appl. Phys. **47**, 7749 (2008).
8. Z. X. Cheng, X. L. Wang, S. X. Dou, K. Ozawa, and H. Kimura, Appl. Phys. Lett. **90**, 222902 (2007).
9. U. Chon, K.-B. Kim, H. M. Jang, and G.-C. Yi, Appl. Phys. Lett. **79**, 3137 (2001).
10. M. E. Villafuerte-Castrejon, F. Camacho-Alanis, F. González, A. Ibarra-Palos, G. González, L. Fuentes, and L. Bucio, J. Eur. Ceram. Soc. **27**, 545 (2007).
11. F. Yang, B. Jia, T. Wei, C. Zhao, Q. Zhou, Z. Li, M. Du, M. Wang, Y. Liu, and C. Xie, Inorg. Chem. Front. **6**, 2756 (2019).
12. A. Huanosta-Tera, R. Castañeda-Guzman, and J. L. Pineda-Flores, Mater. Res. Bull. **38**, 1073 (2003).
13. J. L. Pineda-Flores, E. Chavira, J. Reyes-Garga, A. M. González, and A. Huanosta-Tera, J. Eur. Ceram. Soc. **23**, 839 (2003).
14. S. J. Kim, C. Moriyoshi, S. Kimura, Y. Kuroiwa, K. Koto, M. Takata, Y. Noguchi, and M. Miyayama, Appl. Phys. Lett. **91**, 062913 (2007).
15. A. N. Kalinkin, E. M. Kozhbakhteev, A. E. Polyakov, and V. M. Skorikov, Inorg. Mater. **49**, 1031 (2013).
16. S. A. Ivanov, T. Sarkar, E. A. Fortalnova, E. D. Politova, S. Yu. Stefanovich, M. G. Safronenko, P. Nordbland, and R. Mathieu, J. Mater. Sci.: Mater. Electron. **28**, 7692 (2017).
17. W. Gong and R. Zhang, J. Alloys Compd. **548**, 216 (2013).

18. M. A. Petrova, A. S. Novikova, and R. G. Grebenshchikov, Dokl. Akad. Nauk SSSR **246**, 121 (1979).
19. M. A. Petrova, A. S. Novikova, and R. G. Grebenshchikov, Izv. Akad. Nauk SSSR Neorg. Mater. **18**, 700 (1982).
20. Š. Kunej and D. Suvorov, J. Am. Ceram. Soc. **91**, 3472 (2008).
21. J. Takahashi, K. Kageyama, and T. Hayashi, Jpn. J. Appl. Phys. B **30**, 2354 (1991).
22. G. Garcia-Martinez, L. G. Martinez-Gonzalez, J. I. Escalante-Garcia, and A. F. Fuentes, Powder Technol. **152**, 72 (2005).
23. L. N. Komissarova, V. M. Shatskii, G. Ya. Pushkina, L. G. Shcherbakova, L. G. Mamsurova, and G. E. Sukhanova, *Compounds of Rare Earth Elements. Carbonates, Silicates, Nitrates, Titanates* (Nauka, Moscow, 1984) [in Russian].
24. P. Kostantinov, K. Krezhov, E. Sváb, G. Mészáros, and Gy. Török, Phys. B (Amsterdam, Neth.) **276–278**, 260 (2000).
25. X. Li, W. Wu, F. Liu, Y. Li, P. Si, and H. Ge, Mater. Lett. **118**, 24 (2014).
26. L. V. Morozova, Inorg. Mater. **55**, 295 (2019).
27. V. M. Denisov, L. T. Denisova, L. A. Irtyugo, and V. S. Biront, Phys. Solid State **52**, 1362 (2010).
28. L. T. Denisova, L. A. Irtyugo, Yu. F. Kargin, V. V. Beletskii, and V. M. Denisov, Neorg. Mater. **55**, 516 (2019).
29. *Bruker AXS TOPAS V4: General Profile and Structure Analysis Software for Powder Diffraction Data, User's Manual* (Bruker AXS, Karlsruhe, Germany, 2008).
30. N. A. Lomanova, M. V. Tomkovich, V. L. Ugolkov, and V. V. Gusarov, Russ. J. Appl. Chem. **90**, 831 (2017).
31. C. Long, Q. Chang, and H. Fan, Sci. Rep. **7**, 4193 (2017).
32. M. Takahashi, Y. Noguchi, and M. Miyayama, Jpn. J. Appl. Phys. **41**, 7053 (2002).
33. N. C. Hyatt, J. A. Hriljac, and T. P. Comyn, Mater. Res. Bull. **38**, 837 (2003).
34. M. Takahashi, Y. Noguchi, and M. Miyayama, J. Ceram. Proc. Res. **6**, 281 (2005).
35. Gopalakrishnan, T. Sivakumar, K. Ramesha, V. Thangadurai, and G. N. Subbanna, J. Am. Chem. Soc. **122**, 6237 (2000).
36. C. Capillas, E. S. Tasci, G. de la Flor, D. Orobengoa, J. M. Perez-Mato, and M. I. Aroyo, Z. Kristal. Mater. **226**, 186 (2011).
37. L. T. Denisova, Yu. F. Kargin, L. G. Chumilina, N. V. Belousova, and V. M. Denisov, Inorg. Mater. **56**, 597 (2020).
38. K. Sun, J. H. Cho, F. C. Chou, W. C. Lee, L. L. Miller, and D. C. Johnston, Phys. Rev. B **43**, 239 (1991).
39. C. G. Maier and K. K. Kelley, J. Am. Chem. Soc. **54**, 3234 (1932).

Translated by E. Bondareva